The Optimum Number of Nodes and Radius for Distributed Beamforming Networks

Pongnarin Sriploy[*1],
Peerapong Uthansakul[*2], and **Monthippa Uthansakul**[*3], Non-members

ABSTRACT

This paper presents a ready-made formula to calculate the number of node and network radius for distributed beamforming networks. The calculation is based on guarantee of received signal at destination to be higher than received sensitivity. The proposed calculation model already includes path loss and also imperfection in node location estimation, which can be applied for both indoor and outdoor scenarios.

Keywords: Array signal processing, Distributed beamforming, Path loss, Phase synchronization and Wireless communications.

1. INTRODUCTION

As a rapid increase in data rate transmission in wireless communication is needed, distributed beamforming networks are currently considered as one solution for the next generation of wireless communication systems. The distributed beamforming is based on a random antenna array theory in which all user terminals in the network transmit their same signal at same time to destination or base station [1]. Then, the received signal at destination can be gained when the phase of transmitted signal are aligned following some phase synchronization techniques. According to this concept, the received signal at destination can be gained by $10log_{10}N$, where N stands for the number of collaborative user terminals in the networks. If all user terminals transmit collaborative signal without phase synchronization, the received signal at destination may be not gained as the received signal's phases are off-set. Therefore, phase synchronization is a relatively significant key to obtain maximum beamforming gain. Generally, phase synchronization can be divided into two scenarios according to interaction between nodes and destination: closed-loop and open-loop [2]. For the first concept, destination directly controls the node's phase adjustment by transmitting feedback signal from destination to nodes in which knowledge of distance relative to wavelength between each node and destination is required. According to this, nodes in the networks are able to compensate own phase off-set following the feedback reference signals. Some examples of the mentioned concept have been shown in [3, 4], which are full-feedback closed-loop and one-bit feedback closed-loop synchronization, respectively. For the later concept, the information of node location is required, which can be usually obtained from Global Position System (GPS). Then, nodes in the networks are able to compensate individual phase off-set according to node location information. Some examples of open-loop phase synchronization are master-slave and round-trip open-loop synchronizations as shown in [5, 6]. Comparing between these two scenarios, the open-loop synchronization is more interesting as it does not require any feedback from destination. Unfortunately, utilizing synchronization technique such as one-bit feedback or master-slave gives rise to system complexity at nodes and destination. However, as mentioned before, we can reduce this complexity by utilization of GPS at individual nodes. Then the information of node location can be obtained from GPS directly. Thus, nodes in the networks compensate own phase off-set according to node location information instead of employing phase compensating message though the open-loop concept [7]. However, from literatures, GPS performance standards and specifications indicate an error in location estimation at bound of 95% [8]. As a result, using reference signal from GPS is not a perfect choice. The mentioned error in GPS may come from several causes such as: satellite geometry, satellite orbit, multipath effect or atmospheric effects [9]. Our previous work [10] has shown that the imperfection in node location estimation in terms of radius degrades the gain in the direction of main beam. Also, imperfection in terms of phase makes some changes in main beam direction. However, phase synchronizing error is not the only one factor that affects beamforming performance, but also the path-loss between nodes and destination. The authors of the work presented in [11] have shown that path loss degrades the transmitted signal strength in distributed networks. They have also recommended that an increase in the number of nodes is required to improve the system performance. In addition, the work presented in [12] has also revealed that signal path loss tremendously affects the topology of the networks. Moreover, from

Manuscript received on July 31, 2014 ; revised on December 11, 2014.

* The authors are with Department of School of Telecommunication Engineering, Suranaree University of Technology 111, Mahawittayalai Road, Muang, Nakhon Ratchasima, Thailand 3000 Email: 1D5440054@g.sut.ac.th[1], uthansakul@sut.ac.th[2], mtp@sut.ac.th[3]

our previous work [13], path loss extremely affects beam pattern as it degrades the beamforming gain. At this point, it can be said that phase synchronization and path-loss extremely involve in evaluating the performance of distributed beamforming networks. According to the degradation mentioned above, some researchers have proposed an increase in the number of collaborative nodes and radius of the networks [14, 15]. The reason is that increasing number of collaborative nodes and network radius provides higher beamforming gain. The results have indicated that side lobe level can be reduced when increasing the number of nodes and main beam width is reduced as network radius increases. Unfortunately, an increase in the number of nodes is relatively limited by communication channel and also this introduces an increased budget. Also, the concept of allowing longer network radius may be limited by available space. However, gaining transmitted power is an alternative choice. Still, increasing power in transmitter is also relatively limited because of battery-lifetime constraint. Therefore in this paper, we propose an idea to choose an optimum number of collaborative nodes and network radius for distributed beamforming. The effect of phase synchronizing error and path loos are included to the model. The outcome of study is a ready-made formula to calculate the appropriate number of node and network radius with respect to received sensitivity.

The remainder of this paper is organized as follows. Following introduction, a brief discussion of distributed beamforming and path loss model are shown in Section 2 and 3 respectively. Moreover, the effect of phase synchronizing error in distributed beamforming is discussed in Section 4. Afterwards, the proposed concept for optimum selection of the number of nodes and network radius is presented in Section 5. Finally, Section 6 concludes the paper.

2. DISTRIBUTED BEAMFORMING WITH PERFECT PHASE SYNCHRONIZATION

The distributed beamforming geometry is shown in Fig. 1 which refers to the work presented in [7]. The N collaborative nodes are located in (x, y) plane where k stands for node index ($k = 1, , N$). The node location is uniformly distributed in a specified region. Also, node location is denoted in polar coordinate which is expressed by $r_k = \sqrt{x_k^2 + y_k^2}$ and $\psi_k = tan^{-1}(y_k/x_k)$. Also, destination position is denoted in spherical coordinates by (A, ϕ_0, θ_0). In this work, destination (base station or access point) is assumed at the same plane of other nodes, $\theta_0 = \pi/2$. The node location vectors are $r_k \in [-\pi, \pi]^N$ and $\psi_k \in [-\pi, \pi]^N$. We also assume that each node is equipped with a single isotropic antenna. Also, the mutual coupling effects between nodes are negligible because they are sufficiently separated.

The initial phase of individual node in case of open-loop synchronization referred to x-axis is expressed by

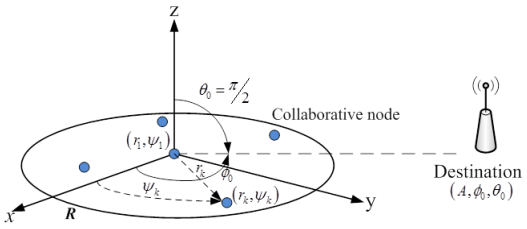

Fig. 1: *Definition of distributed beamforming systems.*

$$\Psi_k = \frac{2\pi}{\lambda} r_k \sin\theta_0 \cos\left(\phi_0 - \psi_k\right) \tag{1}$$

where λ is the wavelength, r_k is distance between k_{th} node and network center. Also, θ_0 and ϕ_0 are direction angles of destination referred to x-axis and z-axis respectively as seen in Fig. 1 while ψ_k is direction angle of k_{th} node referred to x-axis. As considered in far-field region, we assume that each node is located in polar coordinates. Thus, sensor node geometry looks like circular array but location of nodes are random with parameters r_k and ψ_k. Therefore, the far-field array factor of distributed sensor or user terminals can be written as

$$F\left(\phi, \theta | r, \psi\right) \approx \frac{1}{N} \sum_{k=1}^{N} e^{j\frac{2\pi}{\lambda} r_k [\sin\theta_0 \cos(\phi_0 - \psi_k) - \sin\theta \cos(\phi - \psi_k)]} \tag{2}$$

where N is the number of nodes. As we can see in (2), it is similar to circular array factor equation while the node location (r_k, ψ_k) is random. We has previously denoted that destination is located on the same plane with nodes, $\theta = \theta_0 = \pi/2$. Then, (2) can be minimized to

$$\begin{aligned} \tilde{F}\left(\phi | r, \psi\right) &= \frac{1}{N} \sum_{k=1}^{N} e^{j\frac{4\pi}{\lambda} r_k \sin\left(\frac{\phi_0 - \phi}{2}\right) \sin\left(\psi_k - \frac{\phi_0 + \phi}{2}\right)} \\ &= \frac{1}{N} \sum_{k=1}^{N} e^{j4\pi \frac{R}{\lambda} \sin\left(\frac{\phi_0 - \phi}{2}\right) \tilde{r}_k \sin\left(\tilde{\psi}_k\right)} \end{aligned} \tag{3}$$

where R is network radius, $\tilde{r}_k = r_k/R$ and $\tilde{\psi}_k = \psi_k - ((\phi_0 + \phi)/2)$. If network model is a symmetrical circular respected to azimuth angle ϕ, then its array factor does not relate to ϕ_0. To ease the calculation, we also assume that destination direction is at bore sight direction, $\phi_0 = 0°$. Thus, the position of destination is $A, \phi_0 = 0°, \theta_0 = \pi/2$, note that $-\pi \leq \phi \leq \pi$. Then the distributed beamforming array factor from (3) can be minimized to

$$\tilde{F}\left(\phi | z\right) = \frac{1}{N} \sum_{k=1}^{N} e^{-j4\pi \tilde{R} \sin\left(\frac{\phi}{2}\right) z_k} \tag{4}$$

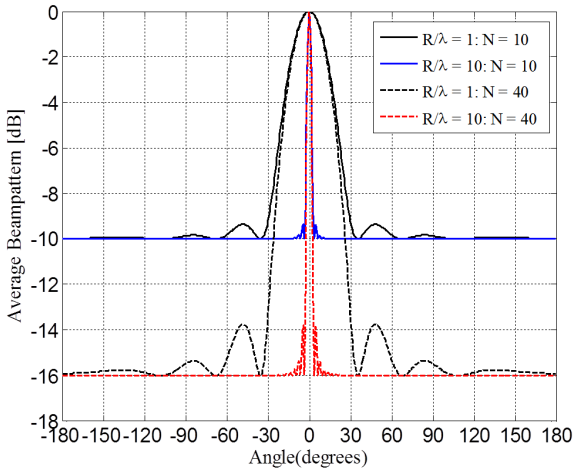

Fig.2: *Average beampattern of distributed beamforming networks with various N and $\tilde{R}$.*

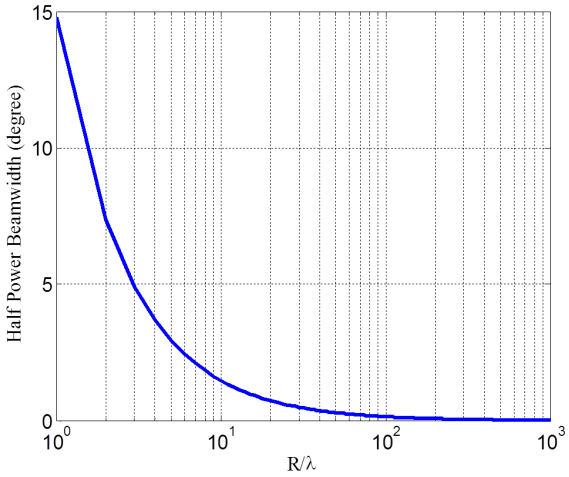

Fig.3: *Half-power beam width of distributed beamforming networks with various network radius $\tilde{R}$.*

where $\tilde{R} = R/\lambda$ is a normalized network radius and corresponding z_k is defined by

$$z_k = \tilde{r}_k \sin\left(\tilde{\psi}_k\right) \tag{5}$$

This z_k has the probability density function (pdf) as follow:

$$f_{z_k}(z) = \frac{2}{\pi}\sqrt{1-z^2}, \qquad -1 \le z \le 1 \tag{6}$$

We can estimate the radiation pattern by taking magnitude of the array factor shown in (4). Then, the far-field radiation pattern is characterized by

$$\begin{aligned} P(\phi|z) &\triangleq \left|\tilde{F}(\phi|z)\right|^2 = \tilde{F}(\phi|z)\,\tilde{F}^*(\phi|z) \\ &= \frac{1}{N^2}\sum_{k=1}^{N}\sum_{l=1}^{N} e^{j4\pi\tilde{R}\sin\left(\frac{\phi_0-\phi}{2}\right)(z_k-z_l)} \\ &= \frac{1}{N} + \frac{1}{N^2}\sum_{k=1}^{N} e^{j\alpha(\phi)z_k}\sum_{\substack{l=1\\ l\neq k}}^{N} e^{-j\alpha(\phi)z_l} \end{aligned} \tag{7}$$

where $\alpha(\phi) = 4\pi\tilde{R}\sin((\phi_0-\phi)/2)$ and ϕ is destination direction in azimuth, within $-\pi \le \phi \le \pi$.

In this paper, nodes positions are assumed to have uniformly random distribution. Thus, we investigate the beamforming performance in terms of average beam- pattern. The average beampattern is expressed by the expectation of far-field beam pattern as follow:

$$P_{av}(\phi) = \mathrm{E}_z\{P(\phi|z)\} \tag{8}$$

where $E_z\{.\}$ is expectation operator. According to (6) and (7), we obtain average beampattern as

$$P_{av}(\phi) = \frac{1}{N} + \left(1-\frac{1}{N}\right)\left|2\frac{J_1(\alpha(\phi))}{\alpha(\phi)}\right|^2 \tag{9}$$

where $J_1(.)$ is first-order Bessel function, N is the number of nodes,$\tilde{R} = R/\lambda$ is normalized network radius and ϕ is destination direction in azimuth. The (9) informs the behavior of average beampattern when the first term of this expression $1/N$ relates to side lobe level. As we can see in Fig. 2, side lobe level becomes lower as the number of nodes N increases. This is because increasing N makes the term of $1/N$ smaller. According to this, side lobe level is only related to the number of nodes while main beam width is related to network radius $\tilde{R}$ in which narrower beam width can be achieved when increasing network radius. This is because main beam width correlates with the second term of (9) or $(1-(1/N))\,|2J_1(\alpha(\phi))/\alpha(\phi)|^2$. When the number of node is very large thus the second term of (9) can be minimized to $|2J_1(\alpha(\phi))/\alpha(\phi)|^2$. Therefore, $\lim_{\alpha(\phi)\to+\infty} |2J_1(\alpha(\phi))/\alpha(\phi)|^2 \approx 0$. Also in (7), $\alpha(\phi)$ is related to network radius . Thus, main beam width can be decreased by increasing network radius $\tilde{R}$. In conclusion, factors N and $\tilde{R}$ appeared in (9) directly relate to beamforming gain of distributed beamforming.

Half-power beam width (HPBW) or 3-dB beam width is the angular separation between the half-power points (or 3-dB) on the antenna radiation pattern, referred to the maximum value of main beam gain. The HPBW of distributed beamforming relates to network radius of collaborative node as discussed before. The HPBW of average beampattern for distributed beamforming can be achieved by numerical solving as shown in (10).

$$\begin{aligned} &\phi_{av}^{3dB} = 2\sin^{-1}\left(\frac{0.1286}{\tilde{R}}\right) \\ &or \quad \phi_{av}^{3dB} = \frac{0.26}{\tilde{R}} \quad when \quad \tilde{R} \gg 1 \end{aligned} \tag{10}$$

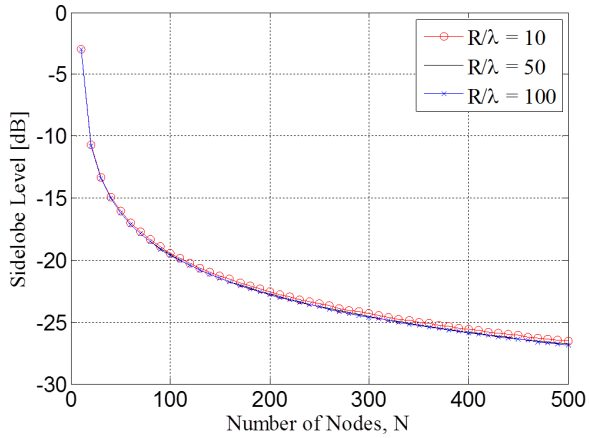

Fig.4: *Side lobe level of distributed beamforming networks with various the numbers of nodes.*

The (10) describes that main beam width inversely depend on network radius. This means that its HPBW can be decreased as network radius increases. This behavior is shown in Fig. 3. On the other hand, increasing network radius is involved side lobe level. Fig. 4 shows simulation result regarding the effect of changing network radius on side lobe level. As we can see, side lobe level of beamforming pattern becomes lower when increasing the number of nodes.

Another important parameter of beampattern is directivity. The directivity informs radiated gain in desired direction referred to single isotropic antenna. The definition of directivity is as follow:

$$D = \frac{U}{U_0} = \frac{\int_{-\pi}^{\pi} P(0)\, d\phi}{\int_{-\pi}^{\pi} P(\phi)\, d\phi} = \frac{2\pi}{\int_{-\pi}^{\pi} P(\phi)\, d\phi} \tag{11}$$

when U is radiation intensity (W/unit solid angle), U_0 is radiation intensity of isotropic antenna (W/unit solid angle) and $P(\phi)$ is radiation intensity in direction of ϕ. A summary equation of directivity from the work presented in [7] is adopted in this paper as follow:

$$D_{av} \geq \frac{N}{1 + 0.09332\frac{N}{\tilde{R}}} \tag{12}$$

Fig. 5 shows the directivity with respect to various the number of nodes and network radius, N and $\tilde{R}$ respectively. As we can see in this figure, directivity is gained as N and $\tilde{R}$ increase. This is because increasing N provides lower side lobe level and increasing $\tilde{R}$ makes its main beam narrower as described in (9). The directivity of distributed beamforming is a parameter to compensate the degradation caused by path loss which will be discussed in next section.

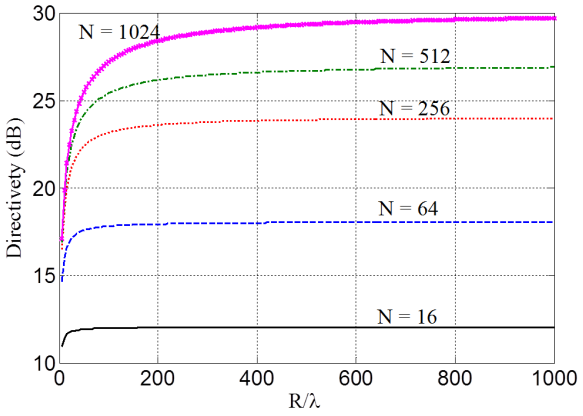

Fig.5: *Directivity of distributed beamforming networks with various N and $\tilde{R}$.*

3. PATH LOSS CHANNEL MODEL

Path loss between user terminals and destination is one significant factor to indicate true performance of the networks. In this paper, we consider path loss for both outdoor and indoor conditions. For outdoor scenario, we assume that transmission between user terminals and destination has no any obstacle causing some scattering or reflecting to the signal. Therefore, we adopt a simple Free-Space Path Loss (FSPL) model presented in [16] which can be expressed by

$$\alpha_k\,(dB) = 20\log_{10}(d_k) + 20\log_{10}(f) - 27.55 \tag{13}$$

where d_k is distance between k^{th} node and destination (meters) and f is operating frequency (megahertz).

We utilize Euclidean estimation for approximating the distance between the k^{th} node and destination, which can be expressed by

$$d_k(\phi,\theta) = \sqrt{A^2 + r_k^2 - 2r_k A\sin\theta\cos(\phi - \psi_k)} \tag{14}$$

where A is distance between network center and destination as shown in Fig. 1, r_k is node location referred to the network center while θ_0 and ϕ_0 are direction angles of destination referred to x-axis and z-axis respectively and ψ_k is direction angle of k^{th} node referred to x-axis as shown in Fig. 1.

When analysing its radiation pattern in far-field region, we usually assume that distance between node and destination is relatively long, $A \gg r_k$. Then, (12) can be minimized to

$$d_k(\phi,\theta) \approx A - r_k\sin\theta\cos(\phi - \psi_k) \tag{15}$$

When the network size is not large, we can estimate that of $d_k(\phi,\theta) \approx A$ which is represented to all node's distance.

In case of indoor condition, we adopt indoor path loss model presented in [17] which has been defined by

$$\gamma_k\,(dB) = 20\log_{10}(f) + 10n\log_{10}(d_k) + L_f(n_f) - 28 \tag{16}$$

Table 1: *Path Loss Exponential, n.*

Frequency [GHz]	Environment		
	Resident	Office	Commercial
0.9	-	3.3	2.0
1.2-1.3	-	3.2	2.2
1.8-2.0	2.8	3.0	2.2
4.0	-	2.8	2.2
60.0	-	2.0	1.7

Table 2: *Floor Penetration Factor, $L_f(n_f)$.*

Frequency [GHz]	Environment		
	Resident	Office	Commercial
0.9	-	9(1floor)	-
	-	19(2floor)	-
	-	24(3floor)	-
1.8-2.8	$4n_f$	$15+4(n_f\text{-}1)$	$6+3(n_f\text{-}1)$

where n is path loss exponent and $L_f(n_f)$ is floor penetration factors. The n and $L_f(n_f)$ can be selected from Tables 1 and Tables 2, respectively.

According to the path-loss model mentioned above, the received signal at destination for outdoor condition can be expressed by

$$R_x = 10\log\left(\frac{N}{1+0.09332}\right) + G_t + G_r + P_t - \alpha_k \qquad (17)$$

when the first term represents distributed beamforming gain (dB), G_t stands for transmitted antenna gain (dB), G_r is received antenna gain (dB), P_t is radiated power (dB) and α_k is path loss in case of outdoor scenario.

Also similar to (17), the received signal at destination for indoor scenario can be expressed by

$$R_x = 10\log\left(\frac{N}{1+0.09332}\right) + G_t + G_r + P_t - \gamma_k \qquad (18)$$

when γ_k is path loss of indoor condition.

Fig. 6 shows degradation in signal strength in case of outdoor and indoor when $n = 3.3$ and $L_f(n_f) = 9$. Please note that both transmitter and receiver are located on same floor. The figure shows that path loss in indoor scenario is more pronounced comparing with the case of outdoor environment. This is because there are many obstacles in indoor environment. This effect has an influence to the performance of distributed beamforming networks. Therefore, the received signal at destination is degraded as revealed in Fig. 7. This figure shows various radiated power levels adopted from [18] including outdoor path-loss effect. As we can see in the figure, received signal strength for all cases is extremely dropped with an increase in distance between destination and nodes. Also, at $A = 1000$ m, received signal strength is approximately -61.3 dBm, -51.3 dBm and -41.3 dBm when radiated power is 0 dBm, 10 dBm and 20 dBm,

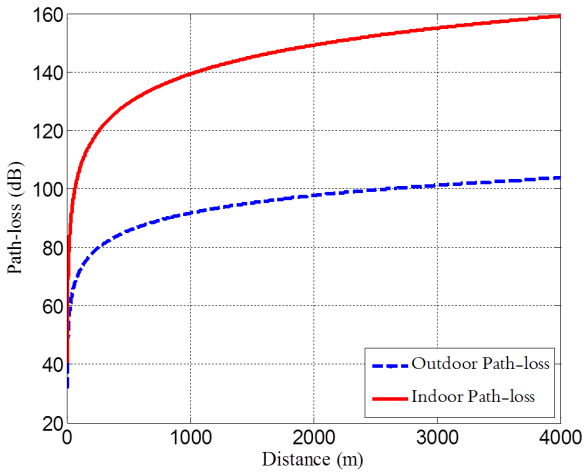

Fig. 6: *FSPL (outdoor and indoor) vs. distance between transmitter and receiver.*

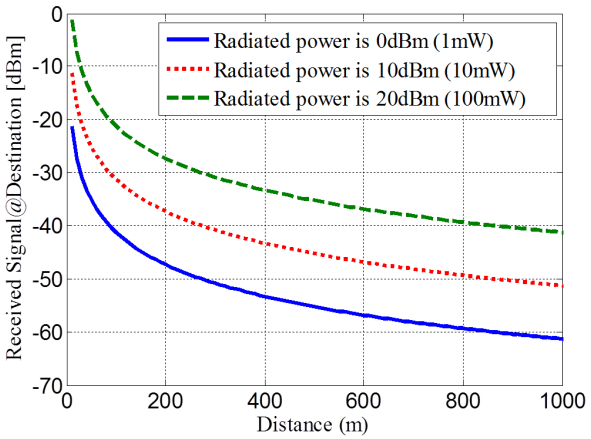

Fig. 7: *Received signal strength at destination in outdoor scenario vs. distance between transmitter and receiver.*

respectively. Next, we further investigate into the effect of path loss on the beamforming performance of distributed beamforming networks.

For outdoor condition, we reveal the effect of path loss on the beamforming performance of distributed beamforming for WSNs. Some utilized parameters appeared from Rochwell Science Center [18] have been adopted. The authors of [18] have developed WSNs for area monitoring and integrated vehicle health management which has several nodes distance. We utilize some parameters from this work as shown in Table 3. Note that all nodes are individually equipped with a single isotropic antenna having identical radiated power.

Fig. 8 shows average beampattern of distributed beamforming networks for outdoor scenario when 40 sensor nodes are randomly located in the networks. Please note that this number is referred to the number

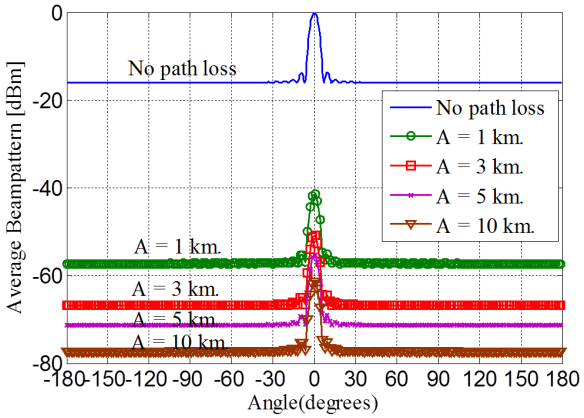

Fig.8: *Average beam pattern in outdoor scenario with several A when number of collaborative nodes (N) is 40 nodes and radiated power is 20 dBm.*

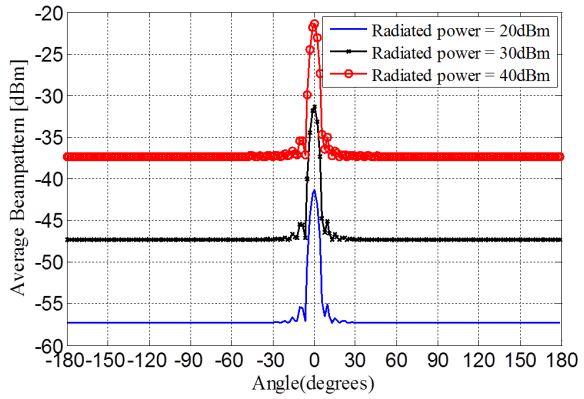

Fig.9: *Simulated average beam pattern in outdoor scenario with several radiated power when number of collaborative nodes (N) is 40 nodes and A is 1000 m.*

of communication channel. As we can see, the effect of path loss is more pronounced when distance (A) between the networks and destination increases. At A = 1 km, the average beampattern is dropped to -40 dBm. At longer distance, the beampattern gain is dropped to -50 dBm, -57 dBm and -62 dBm when A = 3 km, 5 km and 10 km respectively. This is because that path loss effect is more pronounced when distance between transmitter and receiver increases according to (13) and (14).

Fig. 9 shows the average beampattern of distributed beamforming networks when radiated power is given as: 20 dBm, 30 dBm and 40 dBm. The beamforming gain is also degraded with respect to the change of radiated power. As we can see in the figure, beamforming gain is of -43 dBm, -33 dBm and -23 dBm when radiated power is 20 dBm, 30 dBm and 40 dBm, respectively. These results have revealed that path loss effect can be eased by increasing radiated power at transmitter. However, this compensation is

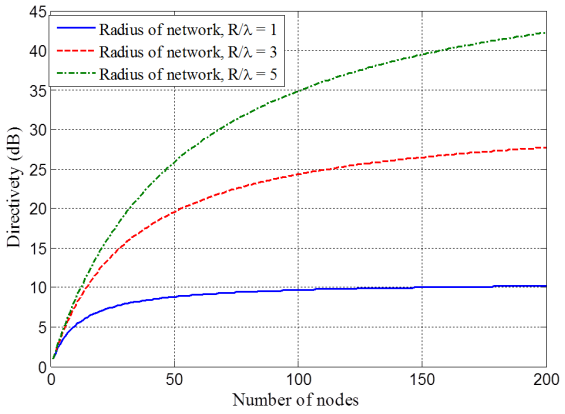

Fig.10: *Beamforming gain vs. the number of collaborative nodes, N.*

not practical when transmitter is far away from receiver. Moreover, this is considerably not practical as the battery-lifetime of sensor nodes is very limited. Nevertheless, some researchers have proposed the idea of increasing the number of nodes to tackle the mentioned problem [12, 14]. Fig. 10 presents that beamforming gain or directivity can be increased when utilizing the higher number of nodes. This is because the beamforming gain or directivity is related to nodes density $N/\tilde{R}$ as shown in (12). However, the obtained directivity is stable when using a large number of nodes. Referring to (12), directivity depends on only $\tilde{R}$ at a large number of nodes, which has been constantly given at the beginning. Also, as seen in Fig. 10, the higher $\tilde{R}/\lambda$ is given then the higher directivity can be obtained. The reason is that directivity reverses to the network radius as shown in (12).

For indoor condition, we adopt simulation model and some parameters from the work presented in [19] which are shown in Table 4. The author of [19] have developed WSNs for home entertainment which is able to send a large data with high speed transmission. The authors have provided a new multithreaded embedded operating system which is integrated with a general purpose single-board hardware platform to enable flexible and rapid prototyping of WSNs.

The results in case of indoor condition look similar to the ones from outdoor condition. As we can see in Fig. 11, the beamforming gain is also extremely dropped by path loss effect especially when distance between WSNs and destination is very far. The beampattern gain is dropped to -47 dBm, -57 dBm and -67 dBm when A = 100 m, 200 m and 300 m respectively. In Fig. 12, radiated power is gained from 30 dBm to 40 dBm and 50 dBm. However, beam pattern gain is still degraded to -32 dBm and -22 dBm, respectively. This seems that gaining transmitted power in indoor cannot overcome the

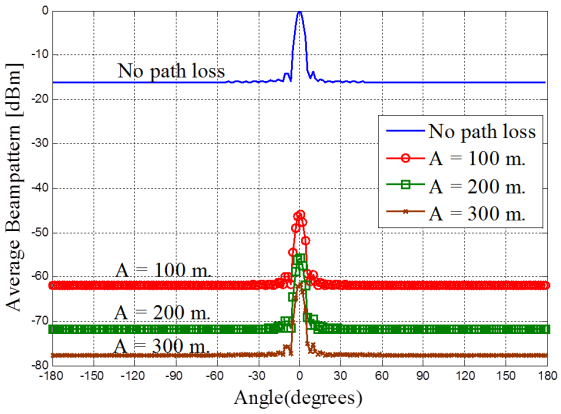

Fig.11: *Average beampattern for indoor scenario with several A when the number of collaborative nodes (N) is 30 nodes and radiated power is 30 dBm.*

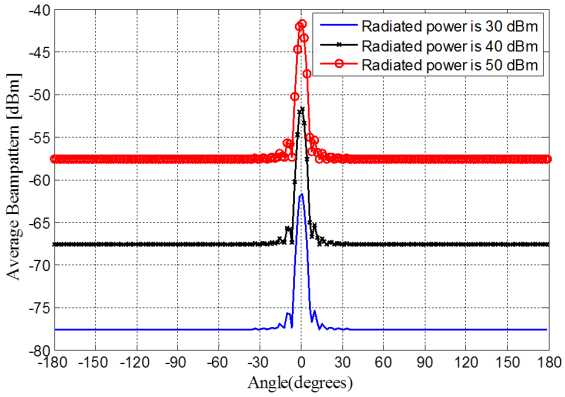

Fig.12: *Average beampattern for indoor scenario with several radiated power when the number of collaborative nodes (N) is 30 nodes and A is 300 m.*

degradation caused by path loss.

From all obtained simulation results, we can conclude that path loss extremely affects the beamforming performance of distributed beamforming systems. There are several remedies such as increasing of network radius or the number of utilized nodes. However, these are considerably not practical. Utilizing more collaborative nodes introduces an increased budget. Also, adding more nodes is not possible for some cases. For example, the work presented in [18] has utilized only 40 nodes operating at the same time as the limitation of available channels. Moreover, an increase in network radius may be limited by the size of available space or environment. However, the path loss is not the only one factor that affects beamforming performance, but also the phase synchronization error or imperfections in node location estimation degrades the beamforming performance. Therefore we step on to discuss an effect of imperfection in node location estimation on distributed beamforming in next section.

4. DISTRIBUTED BEAMFORMING MODEL WITH IMPERFECT PHASE SYNCHRONIZATION

In this work, we focus on open-loop synchronization as it avoids any feedback (or reference) signal from destination. For open-loop scenario, imperfect synchronization due to an error in node-location estimation affects the initial phase presented in (2) as follows:

$$\begin{aligned}\hat{\Psi}_k^{\dagger} &= \frac{2\pi}{\lambda}\left(r_k+\delta r_k\right)\cos\left(\phi_0-\left(\psi_k+\delta\psi_k\right)\right)\\ &= \frac{2\pi}{\lambda}r_k\cos\left(\phi_0-\left(\psi_k+\delta\psi_k\right)\right)\\ &+ \frac{2\pi}{\lambda}\delta r_k\cos\left(\phi_0-\left(\psi_k+\delta\psi_k\right)\right)\end{aligned} \tag{19}$$

where δr_k and $\delta\psi_k$ are estimation error of node location in terms of network radius and angle, respectively. The δr_k and $\delta\psi_k$ are corresponding error random variables where both δr_k and $\delta\psi_k$ are assumed to be independent and identically distributed as well as r_k and ψ_k described in (1). Similar to (7), the beampattern can be expressed by

$$\begin{aligned}P\left(\phi|z,v,\delta\psi\right) &= \left|\tilde{F}\left(\phi|z\right)\right|^2\\ &= \frac{1}{K}+\frac{1}{K^2}\sum_{k=1}^{K}\sum_{\substack{l=1\\l\neq k}}^{K}\\ &e^{-j4\pi\tilde{R}\left\{z_k\sin\left(\frac{\phi-\phi_0-\delta\psi_k}{2}\right)-z_l\sin\left(\frac{\phi-\phi_0-\delta\psi_l}{2}\right)\right\}}\times\\ &e^{j\frac{2\pi}{\lambda}\left(v_k-v_l\right)}\end{aligned} \tag{20}$$

where

$$z_k = \tilde{r}_k\sin\left(\psi_k+\frac{\delta\psi_k}{2}-\frac{\phi+\phi_0}{2}\right) \tag{21}$$

$$v_k = \delta r_k\cos\left(\psi_k+\delta\psi_k-\phi_0\right) \tag{22}$$

We assume that estimation error in network radius δr_k is uniformly distributed over range of $[-r_{max}, r_{max}]$. In addition, estimation error in phase $\delta\psi_k$ is uniformly distributed over range of $[-\psi_{max}, \psi_{max}]$ in constraint between 0 to 2π. The pdf of v_k can be expressed by

$$f_{v_k} = \frac{1}{\pi r_{\max}}\left[\ln\left(1+\sqrt{1-\left(\frac{v}{r_{\max}}\right)^2}\right)-\ln\frac{|v|}{r_{\max}}\right] \quad for\ |v|\le r_{\max} \tag{23}$$

Finally, the average beampattern can be written as

$$P_{av}\left(\phi\right) = \frac{1}{K}+\left(1-\frac{1}{K}\right)\left|A_{\psi}\left(\phi\right)\right|^2\left|A_r\right|^2 \tag{24}$$

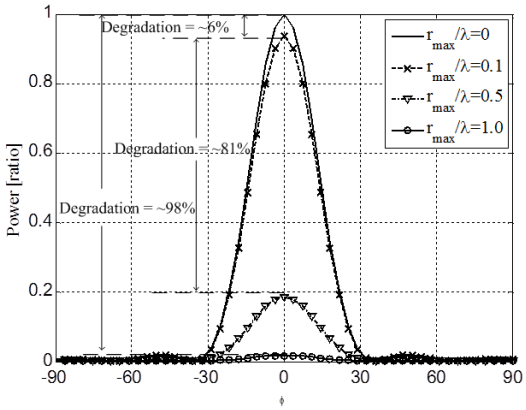

Fig.13: *Average beampattern with imperfection in network radius estimation, r_k.*

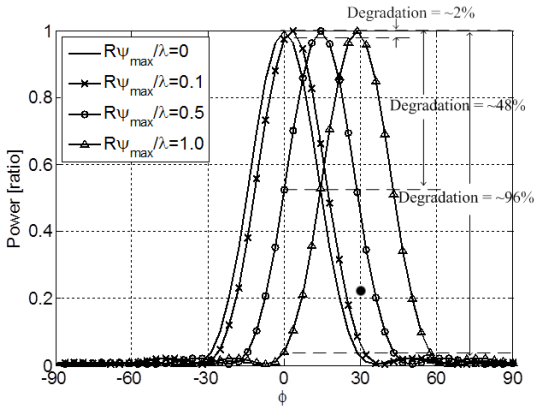

Fig.14: *Average beampattern with imperfection in phase estimation, ψ_k .*

where

$$A_r = E_{v_k}\left\{e^{j\frac{2\pi}{\lambda}v_k}\right\} = \frac{2}{\pi}\int_0^1 \cos\left(\frac{2\pi}{\lambda}r_{\max}t\right)\ln\frac{1+\sqrt{1-t^2}}{t}dt = {}_1F_2\left(\frac{1}{2};1,\frac{3}{2};-\left(\pi\frac{r_{\max}}{\lambda}\right)^2\right) \quad (25)$$

$$A_\psi(\phi) = \mathrm{E}_{z_k,\delta\psi_k}\left\{e^{j4\pi\tilde{R}z_k\sin\left(\frac{\phi_0+\delta\psi_k-\phi}{2}\right)}\right\} = \mathrm{E}_{\delta\psi_k}\left\{\frac{J_1\left(4\pi\tilde{R}\sin\frac{\phi-\delta\psi_k}{2}\right)}{2\pi\tilde{R}\sin\frac{\phi-\delta\psi_k}{2}}\right\} \quad (26)$$

According to this, estimated phase error $\delta\psi_k$ is uniform and distributed over range of $[-\psi_{max},\psi_{max}]$ and $\sin((\phi+\delta\psi_k)/2)\approx(\phi+\delta\psi_k)/2$. Then, we obtain

$$A_\psi(\phi) \approx \frac{1}{2}\left(1-\frac{\phi}{\psi_{\max}}\right) {}_1F_2\left(\frac{1}{2};\frac{3}{2},2;-\left(\pi\tilde{R}(\phi-\psi_{\max})\right)^2\right) + \frac{1}{2}\left(1+\frac{\phi}{\psi_{\max}}\right) {}_1F_2\left(\frac{1}{2};\frac{3}{2},2;-\left(\pi\tilde{R}(\phi+\psi_{\max})\right)^2\right) \quad (27)$$

where ${}_mF_n(x)$ is hypergeometric function. Since the ${}_1F_2\left(\frac{1}{2};\frac{3}{2};-(x)^2\right)=1$ when x=0 and as the function has its symmetrical peak around phase error of $\phi=\pm\psi_{\max}$. Then, the function at main beam center can be defined by

$$A_\psi(\phi=0) = {}_1F_2\left(\frac{1}{2};\frac{3}{2},2;-\left(\pi\frac{R\psi_{\max}}{\lambda}\right)^2\right) \quad (28)$$

From our previous work, we has shown that the imperfection in network radius estimation degrades the gain of main beam while the imperfection in phase estimation deviates the main beam direction [9]. Some examples of imperfection in network radius estimation affecting the gain of main beam are shown in Fig. 13. For this case, the system is assumed to have an error free in phase estimation while estimation error in network radius r_k is assumed as $r_{max}/\lambda = 0.1$, $r_{max}/\lambda = 0.5$ and $r_{max}/\lambda = 1.0$. The obtained results show that the main beam's gain is extremely degraded when error in radius estimation is occurred. The main beam's gain is degraded by 6%, 81% and 98% when estimation error in network radius is $r_{max}/\lambda = 0.1$, $r_{max}/\lambda = 0.5$ and $r_{max}/\lambda = 1.0$, respectively. This is how to calculate the percentage degradation. For example in case of having $r_{max}/\lambda = 0.5$, the ratio of main beam is approximately 0.19 or 19%. Thus, the degradation of main beam's gain is 100-19 = 81% or 0.8.

Furthermore, some examples showing an effect of estimation error in phase are shown in Fig. 14. For this case, estimation of nodes location in terms of radius r_k is assumed to be perfect. Also, estimation error in phase ψ_k are assumed as $R\psi_{max}/\lambda = 0.1$, $R\psi_{max}/\lambda = 0.5$ and $R\psi_{max}/\lambda = 1.0$. The obtained results show that the directions of obtained main beam deviate from the direction of destination ($\phi_0 = 0°$). The deviated main beams are approximately at 3°, 15° and 30°. Thus, the main beam's gain is degraded by 2%, 48% and 96% respectively when comparing to the optimum beamforming. Maximum power ratio of main beam is denoted as 1.0 or 100%. For the case of $R\psi_{max}/\lambda = 0.5$, the ratio of main beam in direction of destination is approximately 0.52 or 52%. Thus, the degradation of main beam's gain is 100-52 = 48% or 0.48. Regarding this simulation results, we can conclude that the imperfection in network radius estimation degrades main beam's gain while the imperfection of phase estimation deviates the direction of main beam.

From running a number of simulations, we have

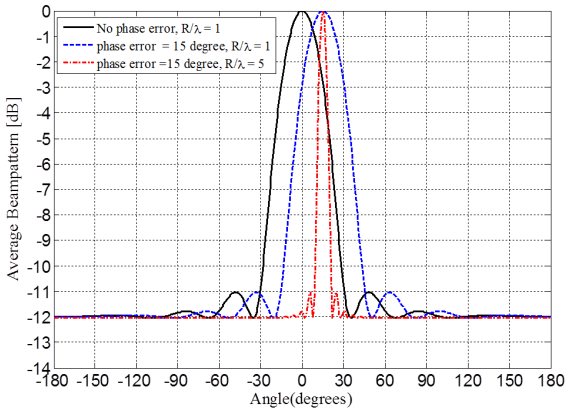

Fig.15: *Average beam pattern with various network radiuses and imperfection of estimated phase, ψ_k.*

found that network radius $\tilde{R}$ is significant parameter for the systems. If utilizing a large network radius is allowed, a small amount of phase error can really affect the system performance as the main beam cannot be pointed to the destination. Some examples are shown in Fig. 15, the number of nodes is set as 16 and direction of destination is given at 0°. Note that in this figure we set an error free to the network radius. The figure shows that, when $\tilde{R} = 1$ and $\psi_{max} = 0.26$, gain at desired direction (0°) drops to -2 dB. In addition, this error is even more pronounced at -12 dB when network radius is wider.

According to simulation results shown in Section 3, path loss and node location estimation error tremendously degrade the beamforming gain of distributed beamforming networks. However, some simulations have revealed that increasing the number of nodes helps improving the beamforming gain. Nevertheless, this is hardly practical because increasing the number of nodes has impact to the system budget. Moreover, utilizing more number of nodes is limited according to available communication channels of the systems. Also an increase in network radius for improving the beamforming gain may be limited by the size of implemented area or environment. The simulation results in Section 4 show that the imperfection in network radius estimation degrades the gain of main beam while the imperfection in phase estimation deviates the direction of main beam. According to those degradation and limitation, we propose an idea to choose the optimum number of collaborative nodes and network radius for distributed beamforming networks in next section.

5. OPTIMUM NUMBER OF NODES AND NETWORK RADIUS

As the limitation of the number of node and accuracy of node location estimation discussed above, we propose the solution to select the optimum number

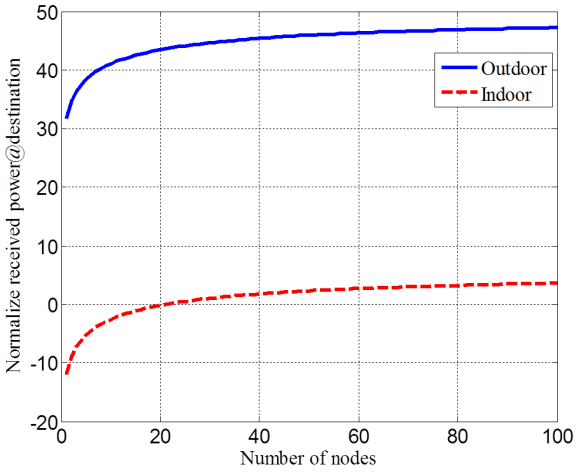

Fig.16: *Normalized received signal strength at destination with various N when $\tilde{R} = 5$.*

of nodes N and network radius R for the distributed beamforming. In this section, we separate the proposed concept into two cases: Perfect Phase Synchronization and Imperfect Phase Synchronization as follows.

5.1 Perfect Phase Synchronization

For this case, synchronization between collaborate nodes and destination is assumed to be perfect. However, beamforming calibration has to be taken place before destination moves out from the main beam for the case of having mobility at destination. When synchronization between nodes and destination is perfect, only path loss between them as mentioned in Section 3 affects beamforming performance. From the (12), (13) and (16), the proposed algorithm for calculating the optimum number of nodes and network radius in case of perfect synchronization is as follow:

$$10\log\left(\frac{N}{1+0.09332}\right) + G_t + G_r + P_t - PL - S \geq 0 \quad (29)$$

when

N = Number of collaborative nodes.
$\tilde{R} = R/\lambda$
G_t = Transmitted gain (dBm)
G_r = Received gain (dBm)
P_t = Sensitivity of destination (dBm)
S = Sensitivity of destination (dBm)
PL = Path loss
f = Operation frequency (MHz)

The objective of proposed formula shown in (29) is to make the received-signal at destination higher than receiver sensitivity at destination. The first term shown in (29) is a distributed beamforming gain or directivity. We herein define the left-side term of (29) as "*normalized received signal*". As a result, we

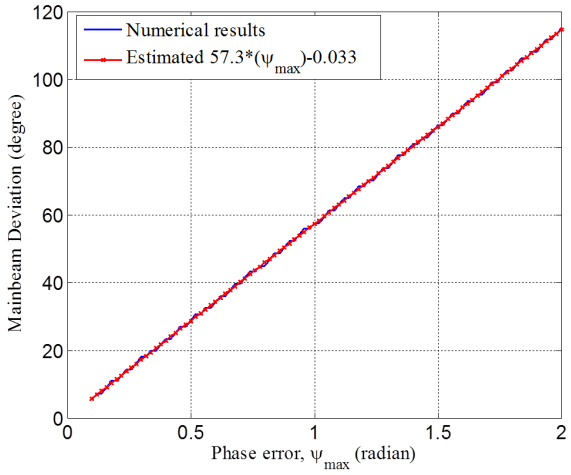

Fig.17: *Numerical and estimated results of main beam deviation vs. estimated phase error, ψ_{max}.*

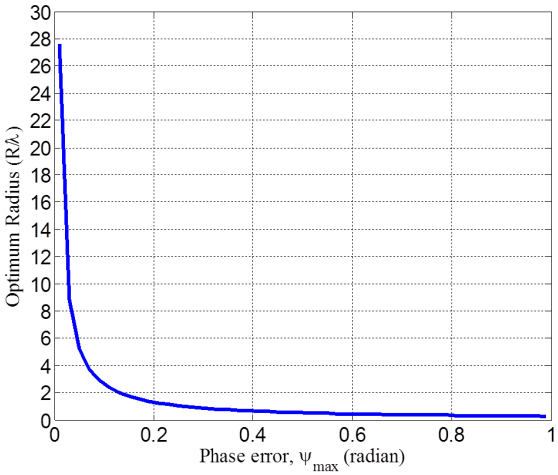

Fig.18: *optimum $\tilde{R}$ vs. estimated phase error, ψ_{max}.*

can select the number of collaborative nods N and network radius $\tilde{R}$ which corresponds to having normalized received signal higher than zero.

Fig. 16 shows some examples to select the proper number of N when $\tilde{R} = 5$. For this case, distance between collaborative networks and destination is assumed as 500 m, path loss in case of outdoor and indoor are -86 dB and -127 dB respectively. The path loss exponent, n is 3.3 and floor penetration factors, $L_f(n_f)$ is 9. Also f is assumed at 916 MHz, P_t is 10 dBm, G_r is 2.5 dBm, G_r is 5 dBm and sensitivity of base station S is -100 dBm. As we can see in this figure, in case of indoor, we should select a number of collaborative nodes N higher than 10 nodes so that destination can receive the transmitted signal having its signal strength higher than receiver sensitivity.

5.2 Imperfect Phase Synchronization

An existent synchronization in distributed beamforming system is often imperfect due to hardware error such as an estimation error in node location employing GPS or phase adjustment error. In this case calculation of the optimum number of N and $\tilde{R}$ is more critical than having perfect phase synchronization as discussed in Section 5.1. Because imperfect estimation in network radius degrades pattern gain while the imperfection in phase estimation deviates main beam direction. Therefore, we separate the proposed algorithm into two steps as follows. For the first step, we carefully select the optimum $\tilde{R}$ in order to maintain its main beam gain not lower than HPBW or -3 dB. Some examples for this case are shown in Fig. 15, when estimated phase error is 0.26 and $\tilde{R}$ is 5, the main beam gain is approximately -12 dB.

Step 1: from (10) and the numerical information shown in Fig. 17, we can find the deviation of main beam comparing to the phase error, ψ_{max}. The numerical results can be obtained from (24) and (28) while the estimated formula of main beam deviation can be taken from this figure as $57.3\psi_{max} - 0.033$. Therefore, the optimum solution is as follows.

$$\begin{aligned} &Main\ \ beam\ \ deviation < Half\ \ Power\ \ Beamwidth \\ &57.3\psi_{\max} - 0.033 < \left(\frac{0.26}{\tilde{R}}\right) \\ &\tilde{R} < \frac{0.26}{57.3\psi_{\max} - 0.033} \end{aligned} \tag{30}$$

The optimum $\tilde{R}$ is selected according to (30) and also Fig.18 informs the optimum value of $\tilde{R}$ when estimated phase error is occurred. For example, if the network has phase error, ψ_{max} of 0.1, then the network radius $\tilde{R}$ must be not higher than 2.5. Note that ψ_{max} is united in radian therefore we multiply (30) with $180/\pi$ for having its unit in degree.

Step 2: Since we get the optimum $\tilde{R}$ from the previous step. Then we consider an imperfect estimation in network radius which degrades the gain of main beam. Therefore we select the optimum N in order to allow the received signal at destination higher than receiver's sensitivity at destination when $\tilde{R}$ is given from Step 1. Finally, the proposed algorithm is as follows.

$$10\log\left(\frac{N}{1+0.09332}\right) L_r + G_t + G_r + P_t - PL - S \geq 0 \tag{31}$$

when L_r is loss factor of main beam degradation by imperfect estimation in radius (ratio) that we describe in Fig. 13. The L_r can be obtained by the information shown in Fig. 13 which shows the main beam degradation caused by imperfect estimation in network radius when r_{max}/λ is given in (25). For example, in case of having $r_{max}/\lambda = 0.5$, the ratio of main beam gain is approximately 0.19 or 19% compared to optimum normalized power of 1 or 100%.

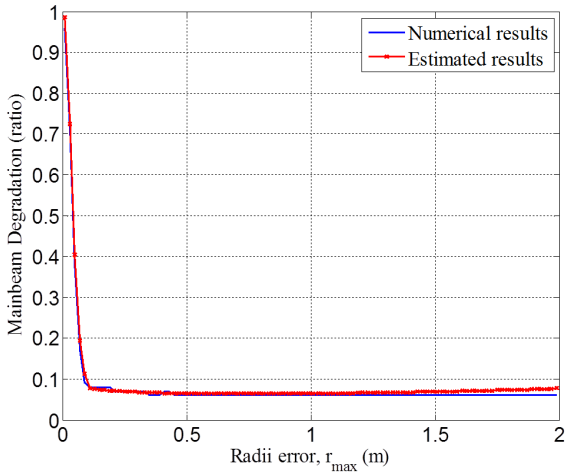

Fig.19: *Relationship between radius error, $r_{max}(m)$ and main beam degradation.*

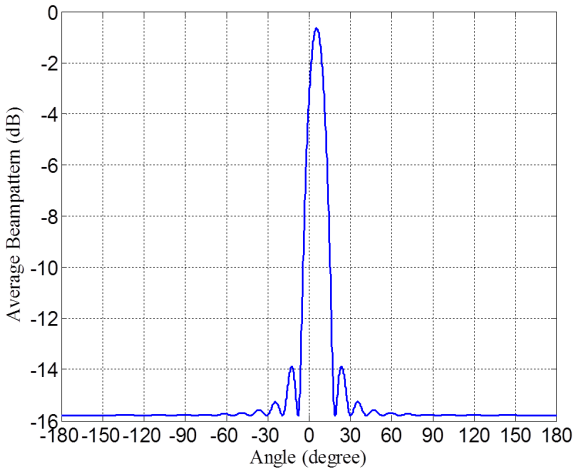

Fig.21: *Average beampattern utilized optimum $N = 38$ and $\tilde{R} = 2.6$ for $\psi_{max} = 0.1$ and $r_{max} = 0.05$.*

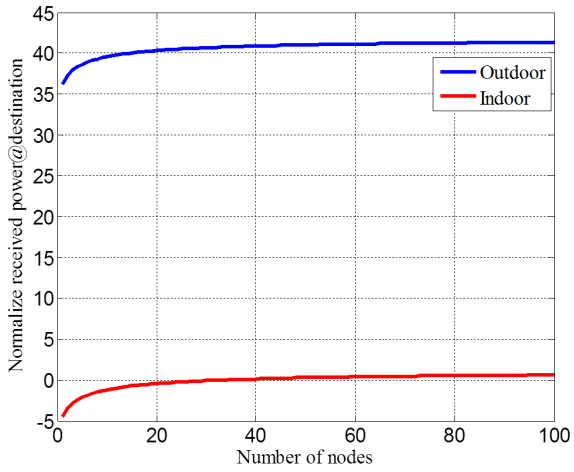

Fig.20: *Normalized received signal strength at destination when $\psi_{max} = 0.1$ and $r_{max} = 0.05$.*

Thus, main beam degradation is 100-19 = 81% or loss factor in main beam degradation caused by imperfect estimation in network radius. Therefore, we obtain L_r is 0.81.

Fig. 19 shows the numerical and estimated results of main beam degradation L_r vs. estimated radius error r_{max}. According to this figure, the estimated values of main beam degradation, L_r is defined as

$$L_r = -39063\,(r_{\max})^4 + 9792\,(r_{\max})^3 - 730\,(r_{\max})^2 + 5(r_{max}) + 1 \tag{32}$$

when $r_{max} \leq 0.1$

$$L_r = 0.084\,(r_{\max})^{-0.09} - 0.025 \tag{33}$$

when $0.1 > r_{max} \leq 0.45$

$$L_r = 0.00091\,(r_{\max})^3 + 0.004262\,(r_{\max})^2 - 0.00671\,(r_{\max}) + 0.066227 \tag{34}$$

when $r_{max} > 0.45$

Finally we obtain the optimum N and $\tilde{R}$ utilizing (30), (31) and (32) to (34) in **Steps 1** and **Steps 2**. For example, we assume the distance between network and destination of 500 m. In addition, f is 916 MHz, P_t is 10 dBm, G_t is 2.5 dBm, G_r is 5 dBm, sensitivity is -100 dBm, path loss exponent, n is 3.3 and floor penetration factors, $L_f(n_f)$ is 9. Moreover phase and radius error are assumed as $\psi_{max} = 0.1$ and $r_{max} = 0.02$ respectively. Firstly, according to (30) or Fig. 18 utilized in **Steps 1**, the optimum $\tilde{R}$ for $\psi_{max} = 0.1$ is not larger than 2.6. Secondly, as the radius error, r_{max} is 0.02, then (32) in **Steps 2** is used to estimate the main beam degradation, thus we obtain $L_r = 0.85$. Finally we obtain the optimum number of nodes, N by using (31). Fig. 20 shows the normalized received signal calculated by (31) in **Steps 2**. As we can see in this figure, we should select N more than 38 nodes for indoor scenario. Therefore, we achieve the average beampattern employing optimum $N = 38$ and $\tilde{R} = 2.6$ as shown in Fig. 21. As we can see in this figure, we obtain the optimum average beam pattern that maintains its main beam gain not lower than HPBW or -3 dB. Moreover, the received signal at destination is also higher than sensitivity of receiver.

6. CONCLUSION

In the existent circumstances, the distributed beamforming performance is degraded by the phase synchronization error and path loss. However, increasing the number of nodes and network radius

in order to obtain higher beamforming gain is constrained. Therefore, this work has proposed the selection for an optimum number of nodes and network radius in order to receive higher signal over receiver's sensitivity at destination. The proposed idea provides ready-made formulas that are helpful for the distributed beamforming designers.

7. ACKNOWLEDGEMENT

The authors acknowledge the financial support from The Royal Golden Jubilee Ph.d Program (RGJ-Ph.D) 1.Q.TS/52/B.1.B.XX and Suranaree University of Technology, Thailand.

References

[1] Y. T. Lo, "A mathematical theory of antenna arrays with randomly spaced elements," *IEEE Trans. Antenna Prog.*, vol. 12, pp. 257-268, May 1964.

[2] R. Mudumbai, D.R. Brown, U. Madhow, and H.V. Poor, "Distributed transmit beamforming: challenges and recent progress," *IEEE Commun. Mag.*, vol. 47, no. 2, pp. 102-110, Feb. 2009.

[3] Y.-S. Tu, and G. J. Pottie, "Coherent cooperative transmission from multiple adjacent antennas to a distant stationary antenna through AWGN channels,"*Proc. IEEE 55th Veh. Tech. Conf.*, vol.1, 2002, pp. 130-134.

[4] R. Mudumbai, "Distributed transmit beamforming using feedback control," *IEEE Trans. Inf. Theory*, vol. 56, no. 1, pp. 411-426, Jan. 2010.

[5] R. Mudumbai, G. Barriac, and U. Madhow, "On the fea-sibility of distributed beamforming in wireless networks," *IEEE Trans. Wireless Commun.*, vol. 6, pp. 1754-63, May 200.

[6] I. Ozil, and D.R. Brown III, "Time-slotted Round-trip carrier synchronization," *Proc. 41st Asilomar Conf. Signals, Syst., Comput.*, 2007, pp. 1781-1785.

[7] H. Ochiai,P. Mitran, H. V. Poor, and V. Tarokh, "Collaborative beamforming for distributed wireless ad hoc sensor networks," *IEEE Trans. Signal process.*, vol. 53, no. 11, pp. 4110-4124, Nov. 2005.

[8] Official U.S. Government information about the Global Positioning System.(2007 Feb, 23). *GPS Performance Standards & Specifications* 1st edition [Online]. Available: http://www.gps.gov/technical/ps/

[9] Ian Poole. *Sources of Errors in GPS* 1st [Online]. Available:http://www.kowoma.de/en/gps/errors.htm

[10] P. Sriploy, P. Uthansakul, and M. Uthansakul, "An effect of imperfection in node location estimation on distributed beamforming", *9th Int. Conf. Elect. Eng./Electron., Comput., Telecommun. Inform. Tech.*, 2012, pp. 1-4.

[11] S. Sfar, G. J. Foschini, R. A. Valenzuela, L. Mailaender, D. Chizhik, K. Karakayali, and R. S. Blum, "Is relayed collaborative communication worth it?," *IEEE Asilomar Conf. Signals, Syst. Comput.*, 2008, pp. 146-150.

[12] A. N. Bishop, and P. N. Pathirana, "On the effect of path loss rates on the optimal receiver position in sensor networks," *IEEE Int. Conf. Inform. Automation*, 2006, pp. 126-128.

[13] P. Sriploy, P. Uthansakul, and M. Uthansakul, "Effect of path loss on the distributed beamforming for wireless sensor networks," *IEEE Int. Conf. Elect. Eng./Electron., Comput., Telecommun. Inform. Tech.*, 2013, pp. 1-4.

[14] A. Kalis, A. G. Kanatas, and G.P. Efthymoglou, "A co-operative beamforming solution for eliminating multi-hop communications in wireless sensor networks," *IEEE J. Selected Areas Commun.*, vol. 28, no. 7, pp. 1055-1062, Sept. 2010.

[15] K. Zarifi, A. Ghrayeb, and S. Affes, "Distributed beamforming for wireless sensor networks with improved graph connectivity and energy efficiency," *IEEE Trans. Signal Process.*, vol. 58. no. 3, pp. 1904-1921, Mar. 2010.

[16] T. S. Rappaport, *Wireless communications: principles and practice*, 2nd ed., Prentice Hall PTR Upper Saddle River, N.J., 2002.

[17] S. Saunders, *Antennas and Propagation for Wireless Communication Systems*, Wiley, 2000.

[18] H. O. Marcy, J. R. Agre, C. Chien, L. P. Clare, N. Romanov, and A. Twarowski, "Wireless sensor networks for area monitoring and integrted vehicle health management applications," *Proc. AIAA Guidance, Navigation, and Control Conf. Exhibit*, 1999, pp. 1-10.

[19] H. Abrach, J. Carlson, H. Dai, J. Rose, A. Sheth, B. Shucker, and R. Han , "MANTIS: system support for MultimodAl NeTworks of In-situ Sensors," *Proc. 2nd ACM Int. Workshop Wireless Sensor Networks Applicat.*, 2000, pp. 50-59.

Pongnarin Sriploy received the B.S. and M.S.degree in telecommunication engineering from Suranaree Univaersity of Technology, Nakhon Ratchasima, Thailand, in 2007 and 2009, respectively. He is currently pursuing the Ph.D. degree in telecommunication engineering at Suranaree Univaersity of Technology. From 2009 to 2011, he was a product engineer at Seagate Technology (Thailand) Ltd. His research interest includes the smart antenna and distributed beamforming.

Peerapong Uthansakul received the B.Eng and M.Eng of Electrical Engineering from Chulalongkorn University, Thailand, in 1996 and 1998 respectively, and Ph.D. degree (2007) in Information Technology and Electrical Engineering from The University of Queensland, Australia. From 1998 to 2001, he was employed as a telecommunication engineer at the Telephone Organization of Thailand. At present, he is working as Associate Professor in School of Telecommunication Engineering, Suranaree University of Technology, Thailand. His research interests include wave propagation modelling, MIMO, OFDM and advance wireless communications.

Leonardo L. Bravo-Roger received the B.Eng degree (1997) in Telecommunication Engineering from Suranaree University of Technology, Thailand, M.Eng degree (1999) in Electrical Engineering from Chulalongkorn University, Thailand, and Ph.D. degree (2007) in Information Technology and Electrical Engineering from The University of Queensland, Australia. She received 2nd prize Young Scientist Award from 16th International Conference on Microwaves, Radar and Wireless Communications, Poland, in 2006. At present, she is lecturer in School of Telecommunication Engineering, Suranaree University of Technology, Thailand. Her research interests include wideband/narrowband smart antennas, automatic switch beam antenna, DOA finder, microwave components, application of smart antenna on WLANs.